Application of Machine Learning in Reconstructing Aqueous Muons

July 03, 2026

Shuo Ma

Contents

01 / Background and Motivation

02 / Simulation and Data Preprocessing

03 / Machine Learning Models & Performance on Simulated Datasets

04 / Muon Direction Reconstruction Based on Measured Experimental Data

05 / Conclusion and Future Work

1 Background and Motivation

Motivation

1. The underground detection environment of the Jinping facility contains **particle scattering** and **background noise**, imposing stringent requirements on muon angular reconstruction performance.

2. The machine learning accuracy is excellent. ML algorithms can automatically capture scattering and noise signals as **latent features**, delivering strong robustness across diverse detection scenarios.

aspect	machine learning
Principle	data drive
Precision	high
Speed	fast
Data requirement	high
Robustness	strong

Detector structure

Outer Tank Shell

Simplified Supporter Structure

Water

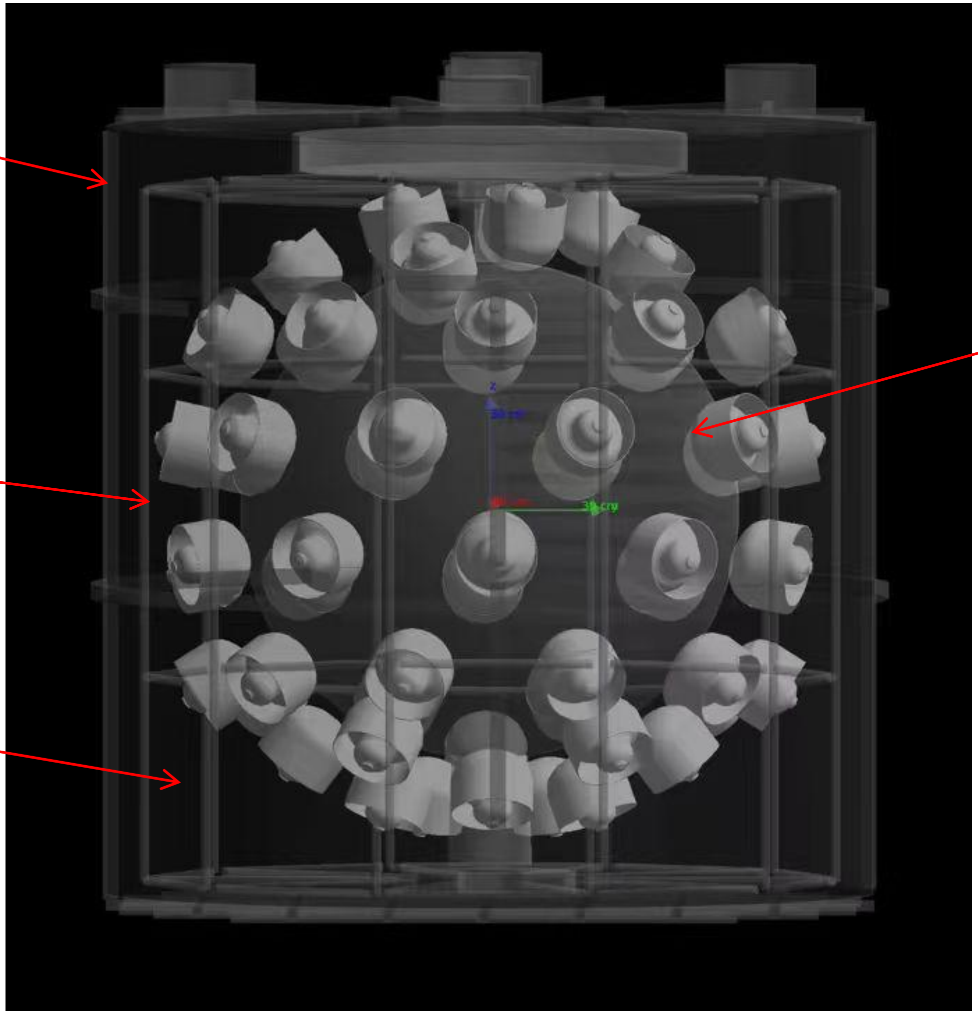

LS Target

2 Simulation and Data Preprocessing

Incidence Simulation

Muon simulation is performed using the JSAP program, where muons penetrate the New_1t_Water_Rock10 detector vertically from top to bottom to produce ROOT-format data files.

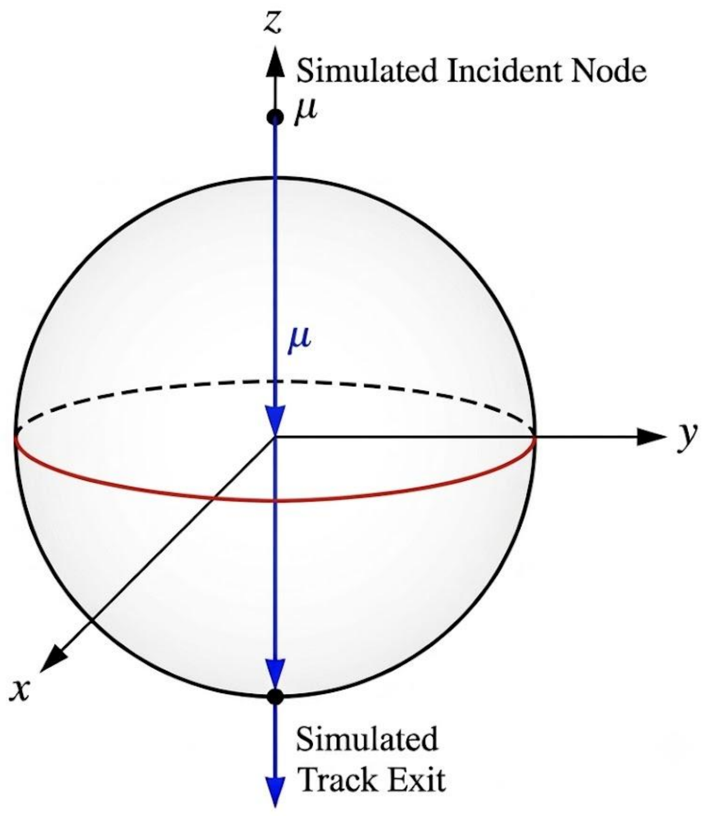

1. **Baseline Calculation**: The average value of the first 100 sampling points per channel is defined as the signal baseline.

2. **Threshold Definition**: threshold = baseline − 5.

3. **Trigger Time T**: The timestamp where the signal first crosses below the threshold is extracted and refined via linear interpolation.

4.**Deposited charge Q**:

Q=300×baseline−raw signal

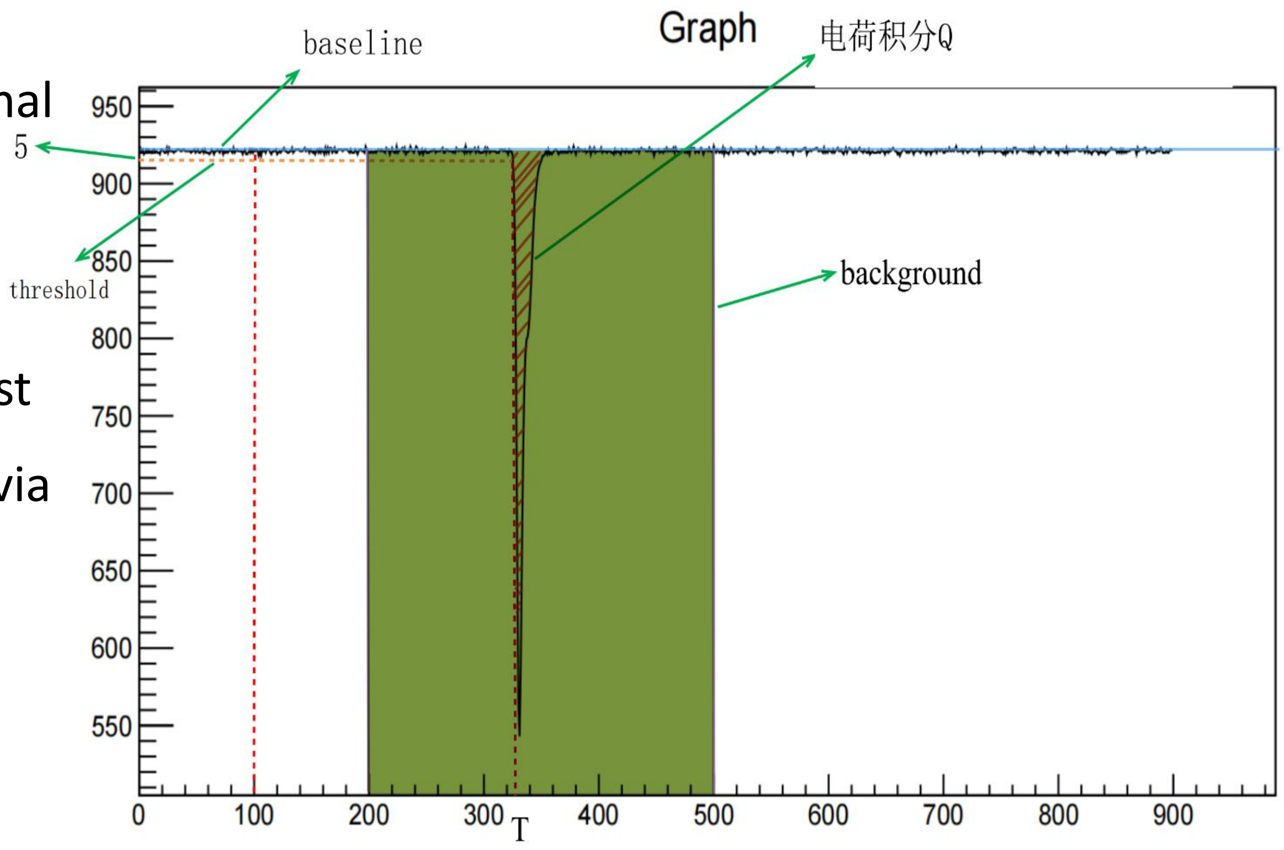

Simulated Data: Muons Incident from Top to Bottom

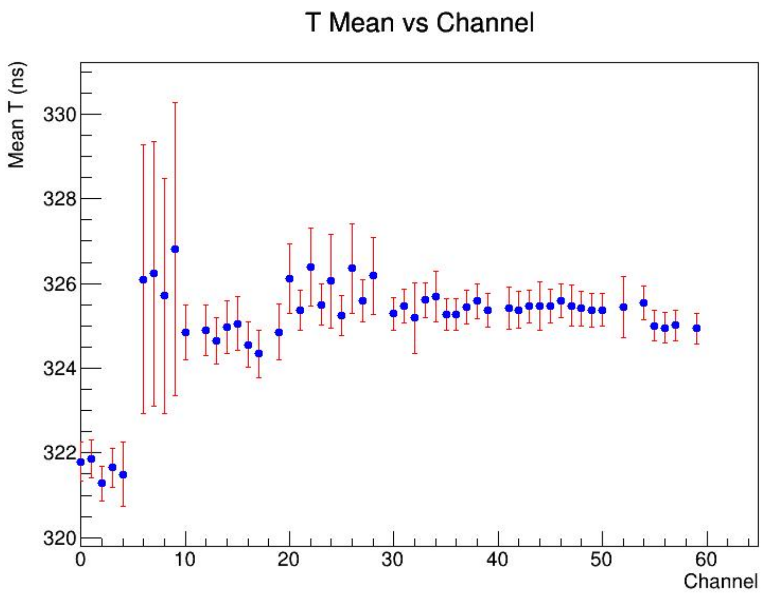

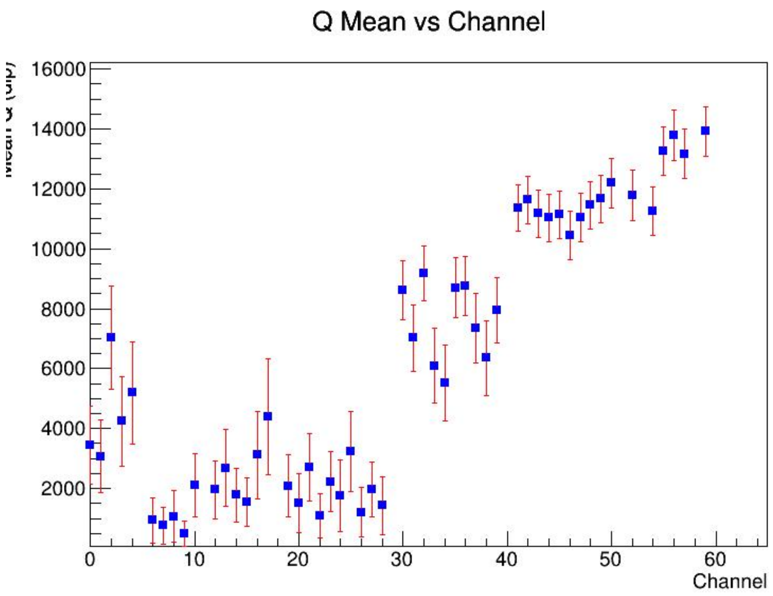

- The average trigger delay of the first 5 channels is significantly lower.
- For channels with channel number ≥ 30, the average amount of collected charge is significantly increased.

Simulated Data: Muons Incident from Bottom to Top

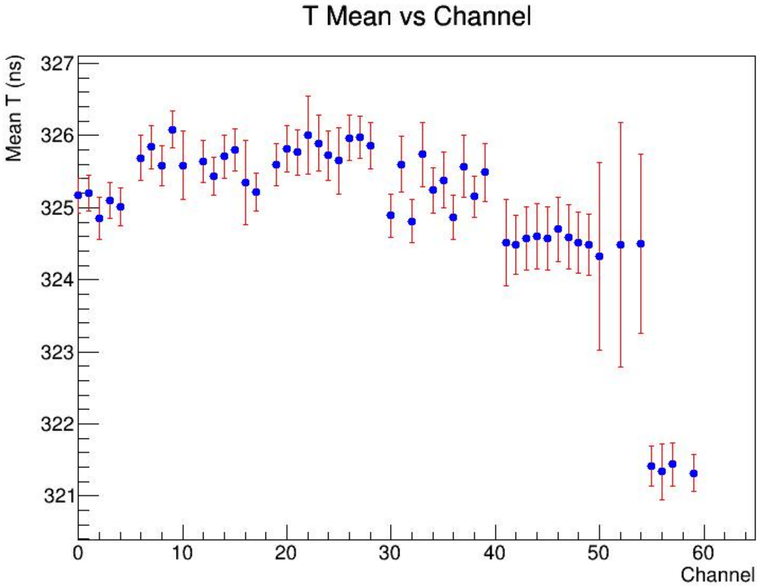

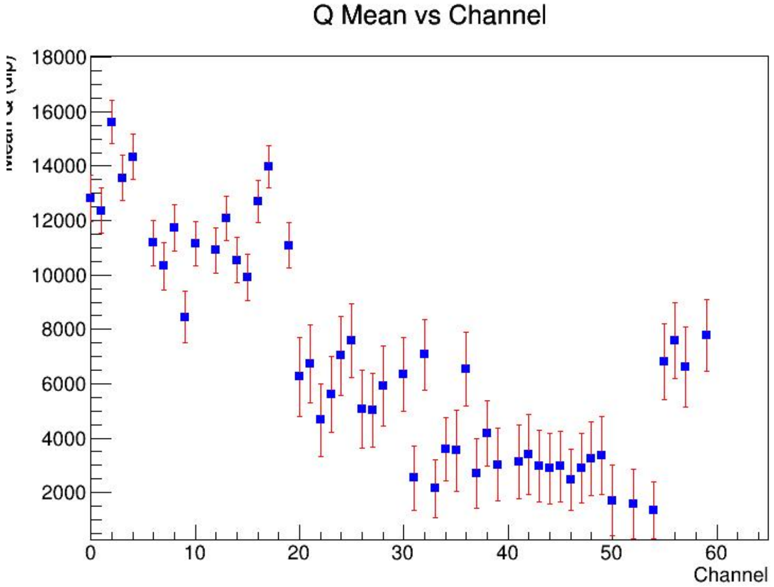

- For muons propagating in the reverse incident direction, the variation trends of observables T and Q are **fully reversed**. Upward-incident muons yield **earlier** trigger time T due to **earlier signal arrival**, together with larger deposited charge Q resulting from extended photon propagation paths.
- Observables **T** and **Q** provide sufficient discrimination of muon incident directions and serve as valid i**nput features** for ML-based angular reconstruction.

3 Machine Learning Models & Performance on Simulated Datasets

Comparative Analysis of Model Mean Absolute Error under Different Feature Input Schemes

兰州大学 | LANZHOU UNIVERSITY

T

θ Mean Absolute Error: 4.43°
ϕ Mean Absolute Error: 6.93°

Q

θ Mean Absolute Error: 3.48°
ϕ Mean Absolute Error: 4.91°

T+Q

θ Mean Absolute Error: 2.31°
ϕ Mean Absolute Error: 3.91°

MAE=|*angle_pre - angle_truth*|*(1/*n*)

MLP

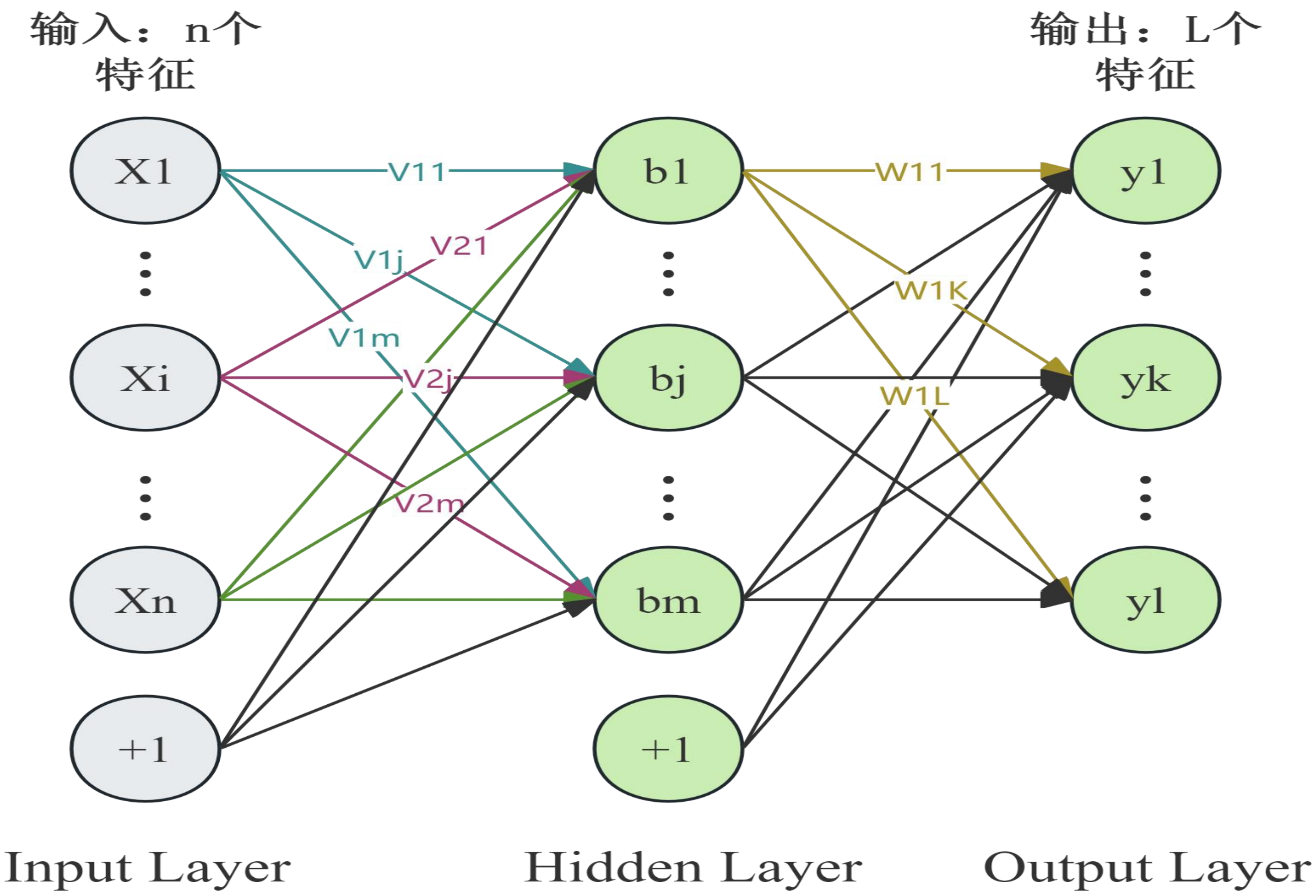
输入：n个
特征
输出：L个
特征
X1
Xi
Xn
+1
b1
bj
bm
+1
y1
yk
yl
V11
V1j
V21
V1m
V2j
V2m
W11
W1K
W1L
Input Layer
Hidden Layer
Output Layer

MLP 3D Angle Prediction Error Analysis

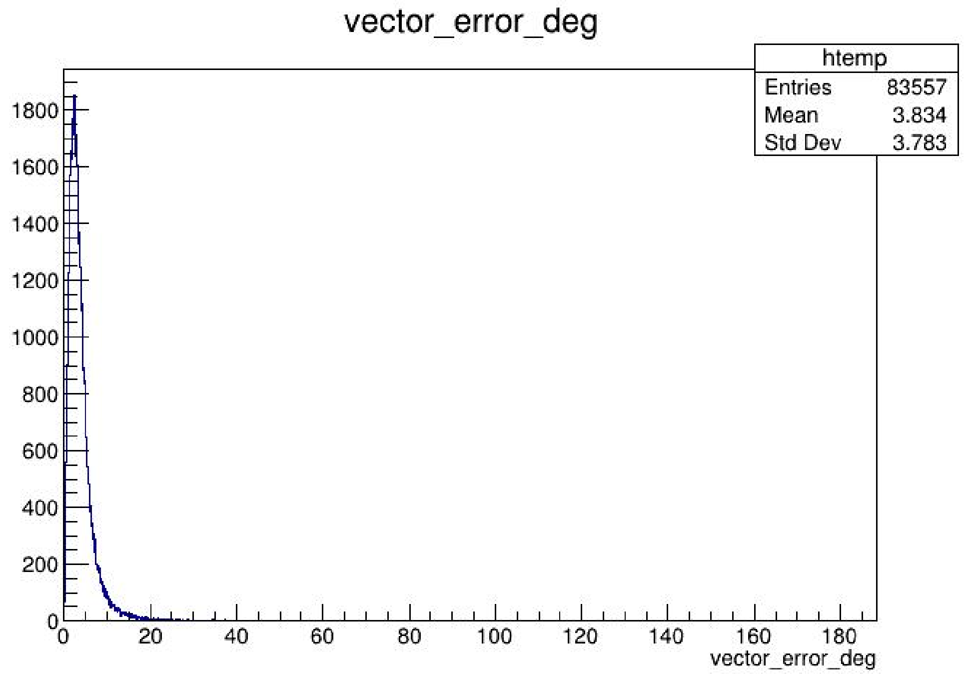

68th percentile: 4.08°

The model controls the 3D pointing deviation within 4.08° for 68% of the events, with an average deviation of 3.834°.

CNN

Neuron

Input signal

Output signal

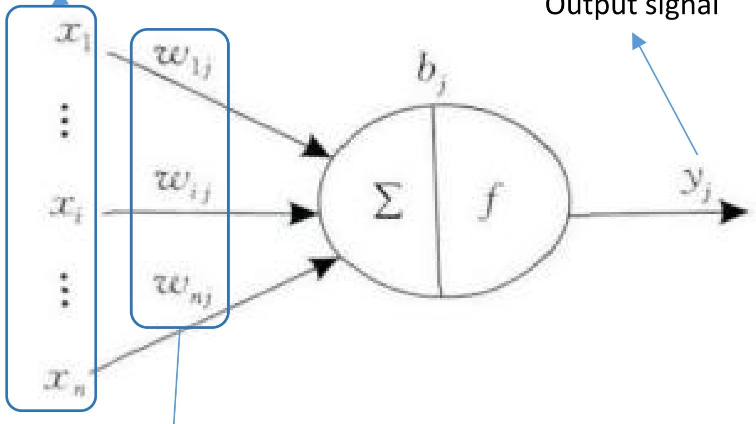

Connection weight

$$y_j = f\left(b_j + \sum_{i=1}^{n}(x_i \times w_{ij})\right)$$

$$x_m^t = b_m^t + \sum_{i=1}^{k} \omega_{im}^{t-1} \times y_i^{t\text{-}1}$$

$$y_m^t = f(x_m^t)$$

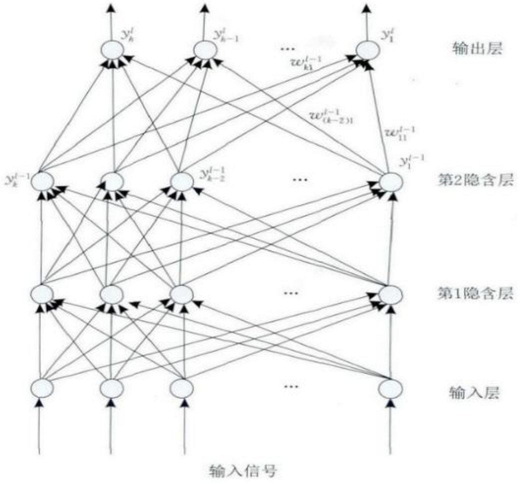

Multilayer Perceptron

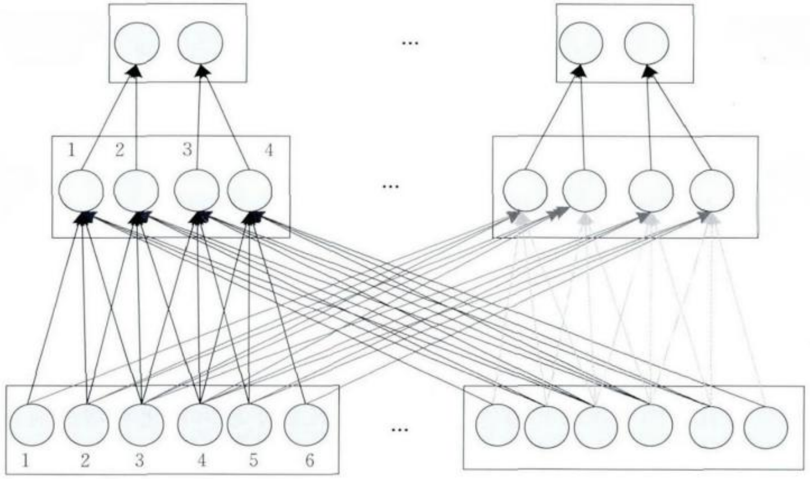

CNN 3D Angle Prediction Error Analysis

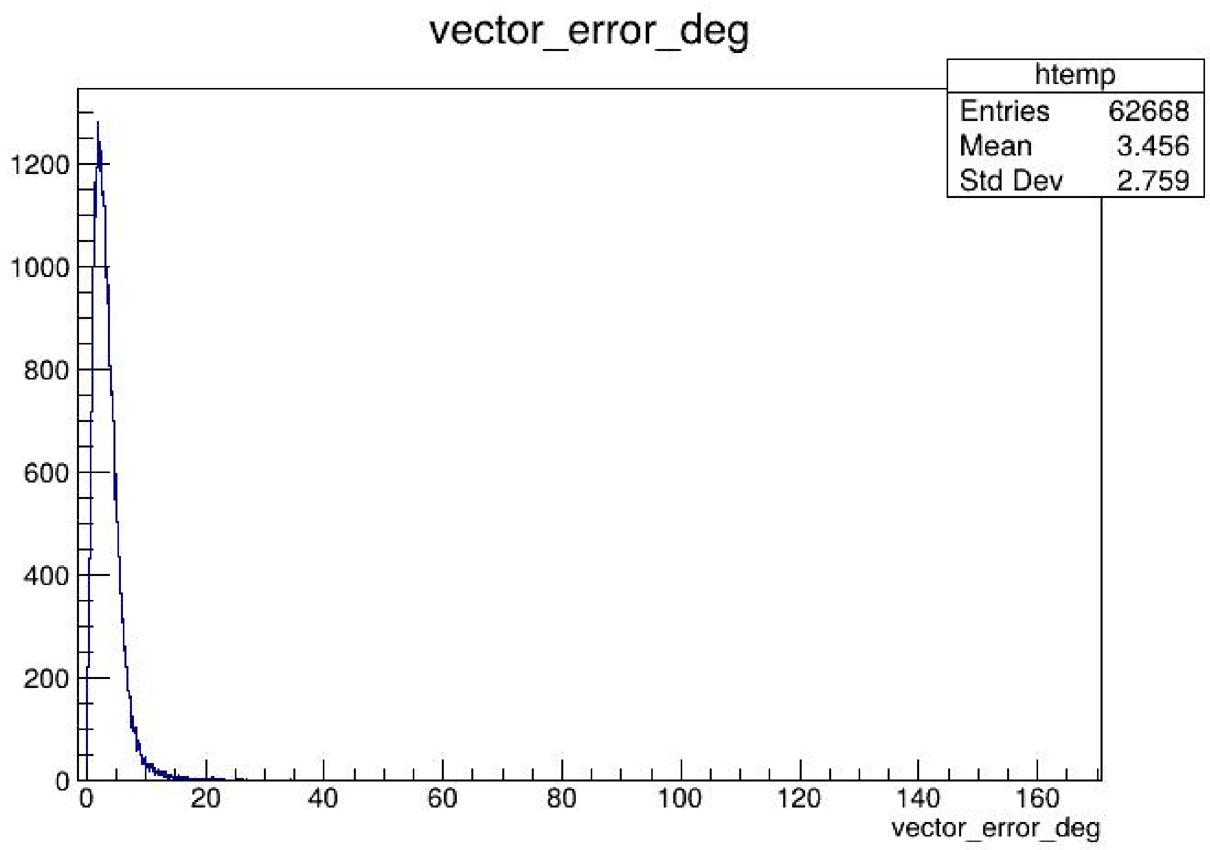

68th percentile: 3.95°

The model controls the 3D pointing deviation within 3.95° for 68% of the events, with an average deviation of 3.45°.

HEALPix-CNN 3D Angle Prediction Error Analysis

Directly map the PMT data to the HEALPix spherical pixels. HEALPix pixels are assigned explicit spherical longitude and latitude coordinates. Under the NESTED indexing scheme, pixel connectivity strictly conforms to the spherical hierarchical partitioning structure.

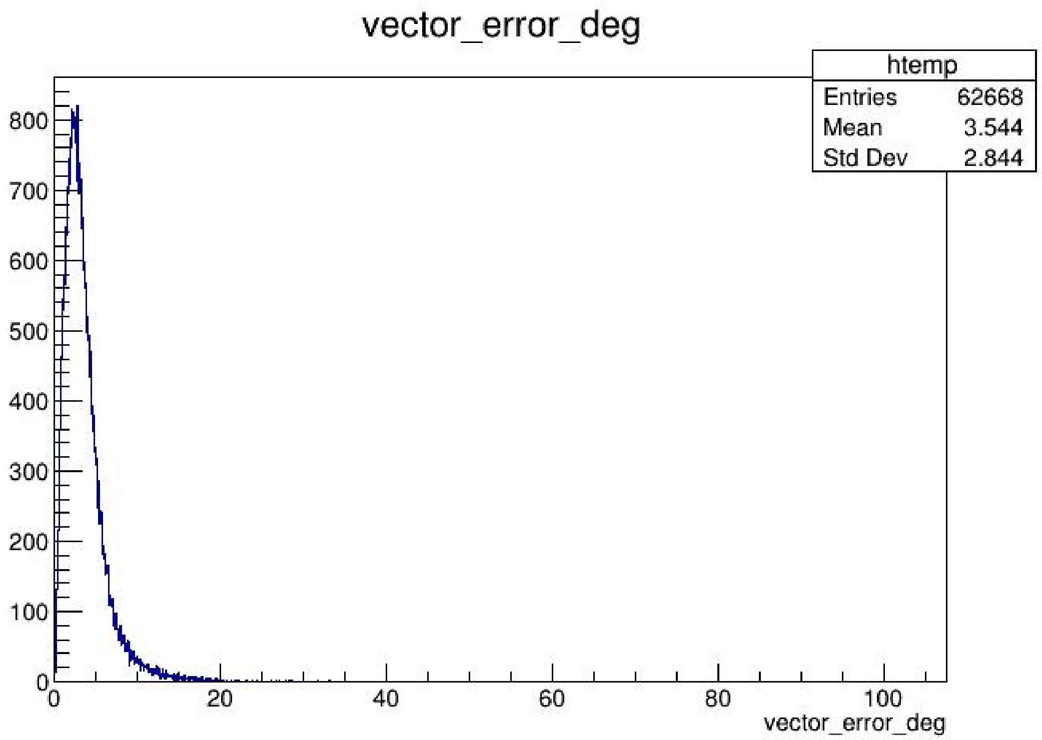

68th percentile: 3.92°

The model controls the 3D pointing deviation within 3.92° for 68% of the events, with an average deviation of 3.54° .

Decision Tree & Random Forest

Decision Tree

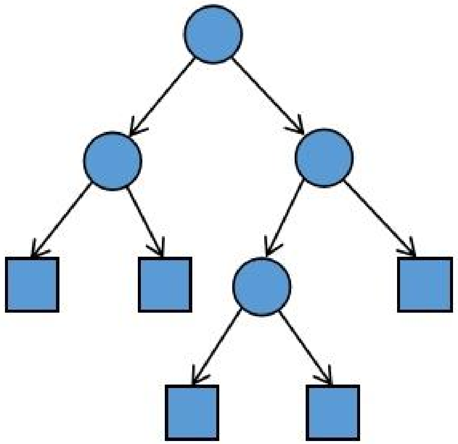

Random Forest

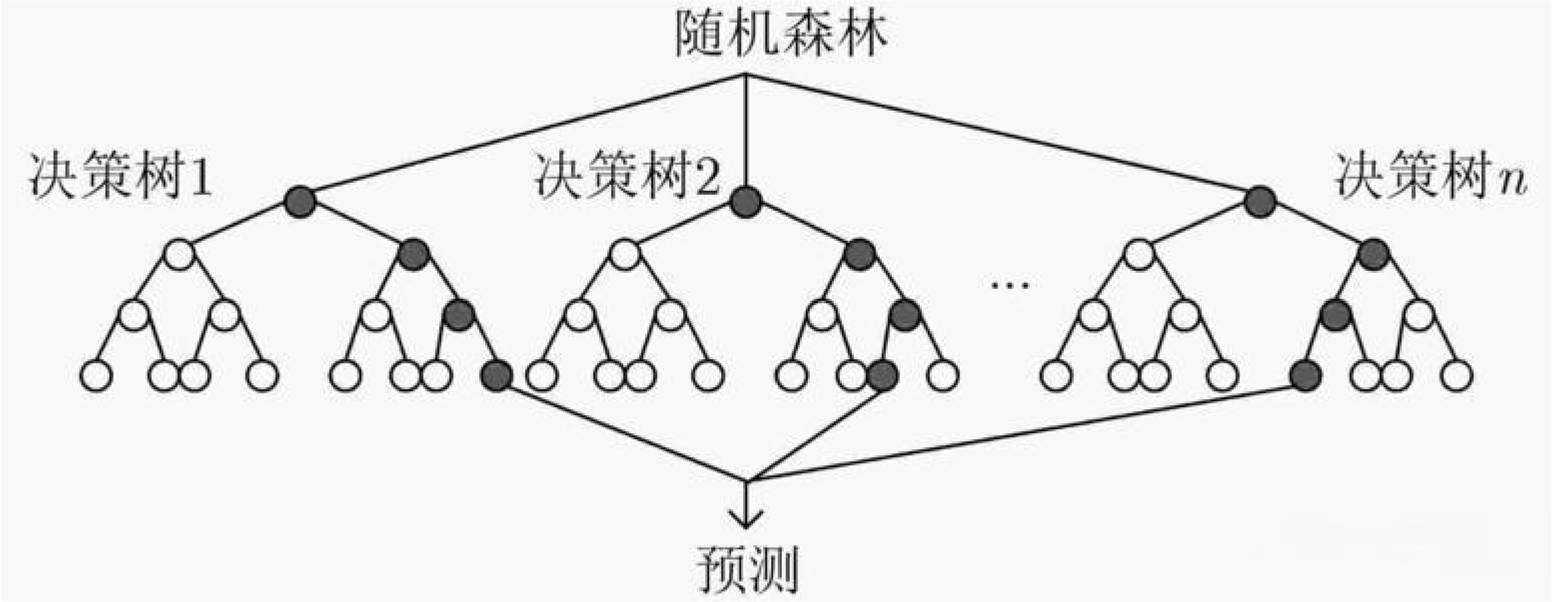

Decision Tree Test Set 3D Angle Prediction Error Analysis

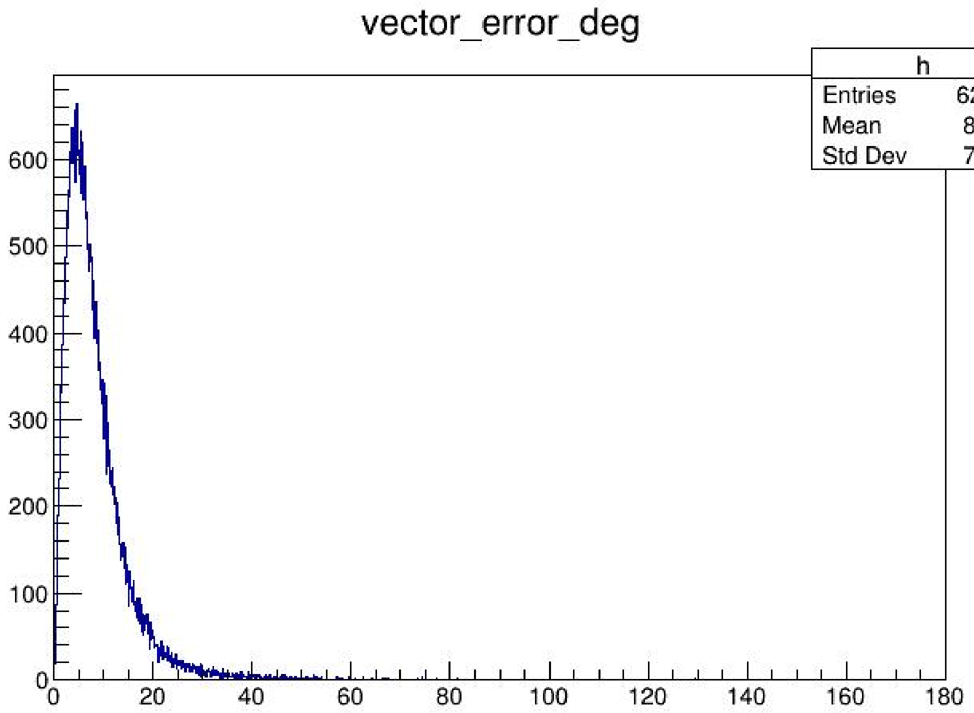

68th percentile: 9.09°

The model controls the 3D pointing deviation within 9.09° for 68% of the events, with an average deviation of 8.33°.

Randomforest 3D Angle Prediction Error Analysis

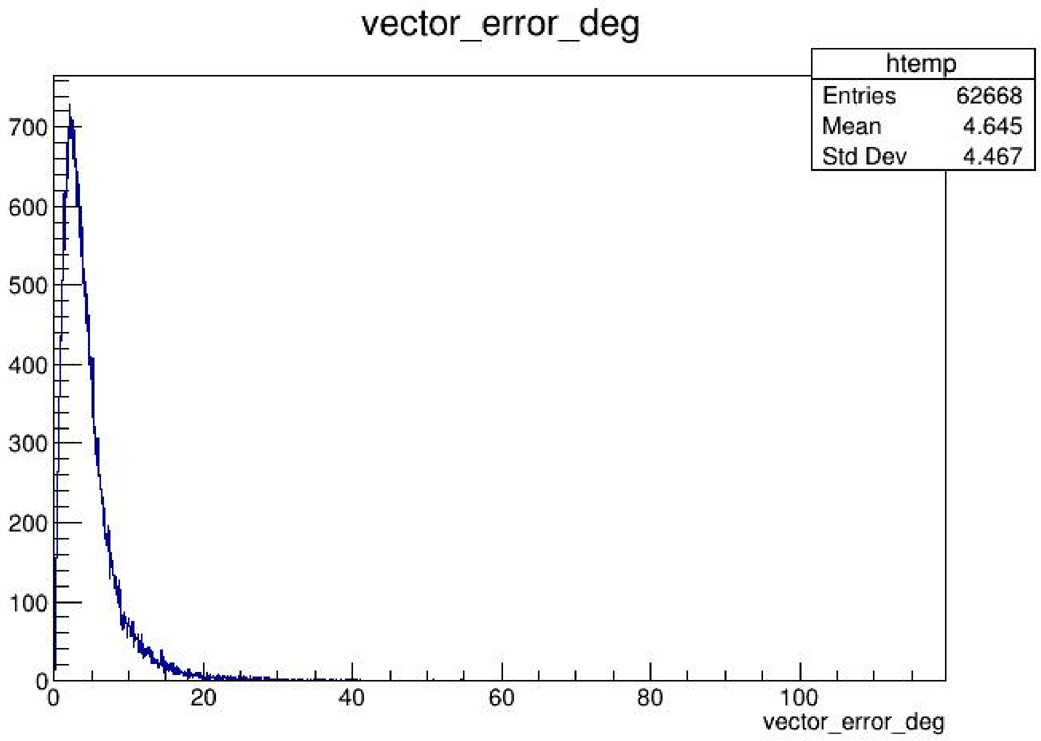

68th percentile:4.93°

The model controls the 3D pointing deviation within 4.93° for 68% of the events, with an average deviation of 4.64°.

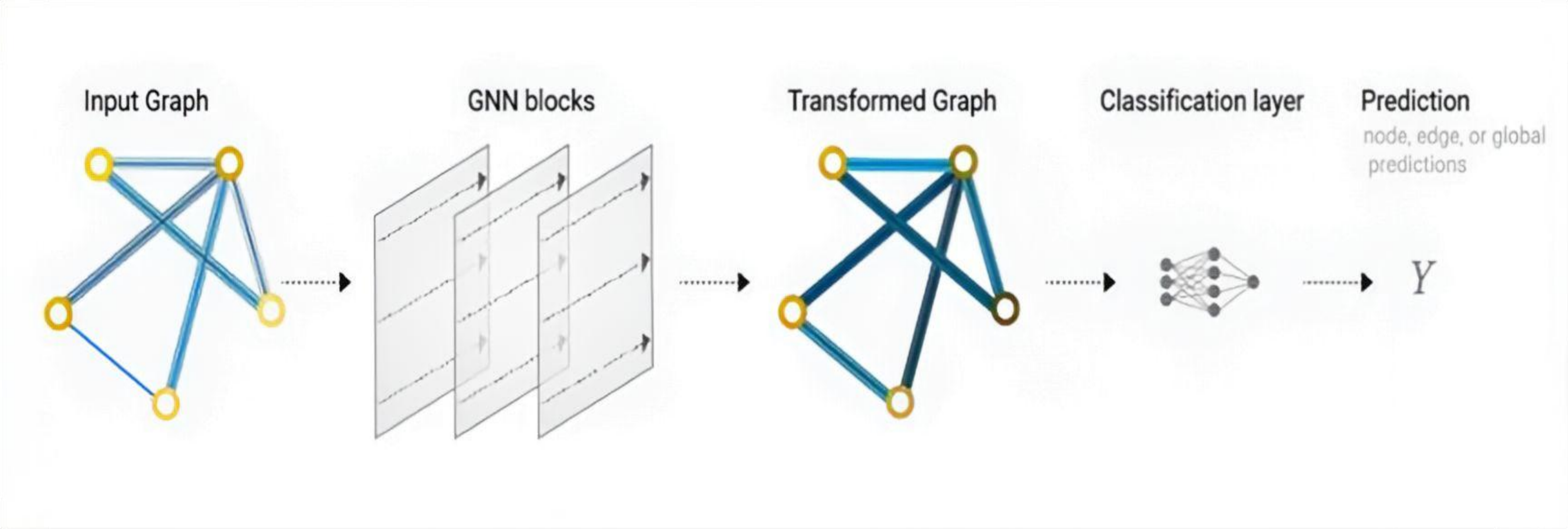
Input Graph
GNN blocks
Transformed Graph
Classification layer
Prediction
node, edge, or global predictions
Y

GNN 3D Angle Prediction Error Analysis

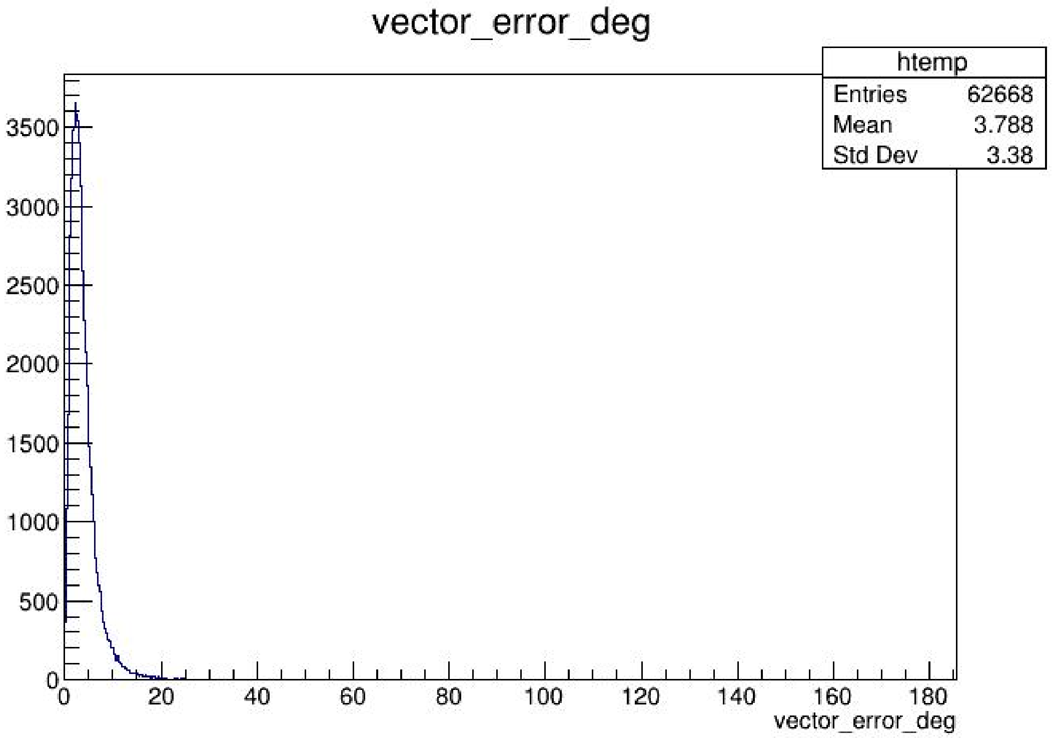

68th percentile:4.15 °

The model controls the 3D pointing deviation within 4.15° for 68% of the events, with an average deviation of 3.79°.

DeepSphere

1.Dimensionality reduction and noise reduction

2.Enlarge the receptive field

3.Reduce computational complexity

Perform the final global convolution to extract directional features.

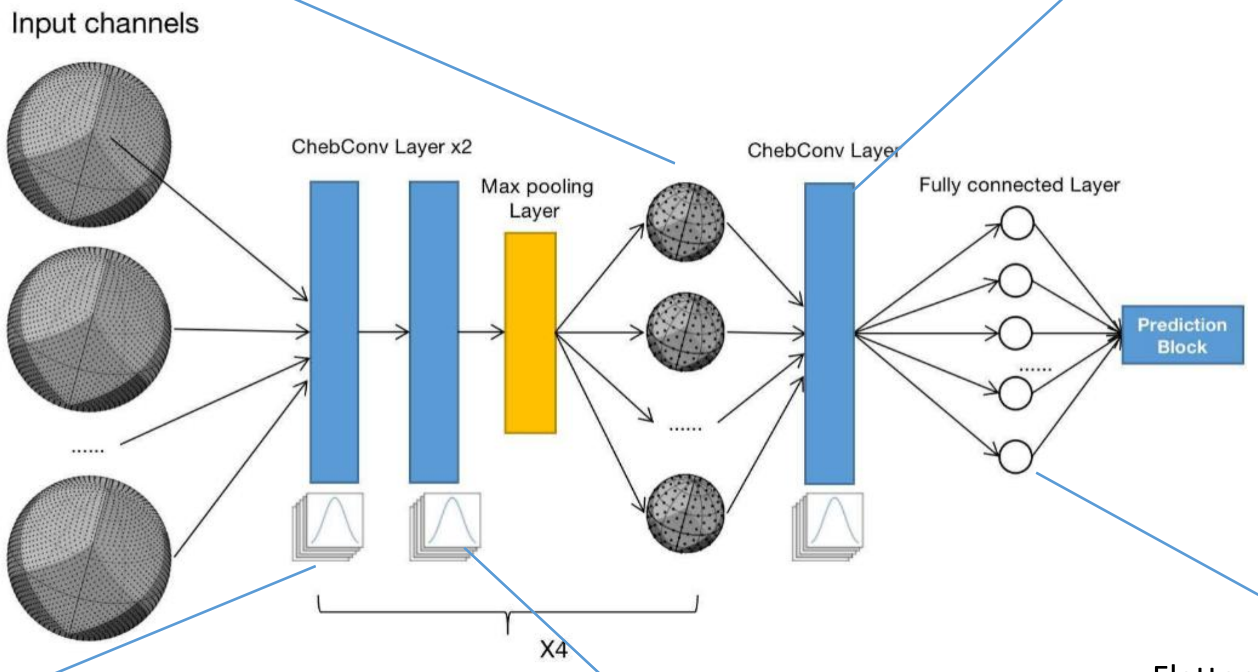

Extract higher-dimensional global features

Extract local low-dimensional features

Flatten the 2D spherical features into a 1D feature vector

DeepSphere 3D Angle Prediction Error Analysis

蘭州大學 | LANZHOU UNIVERSITY

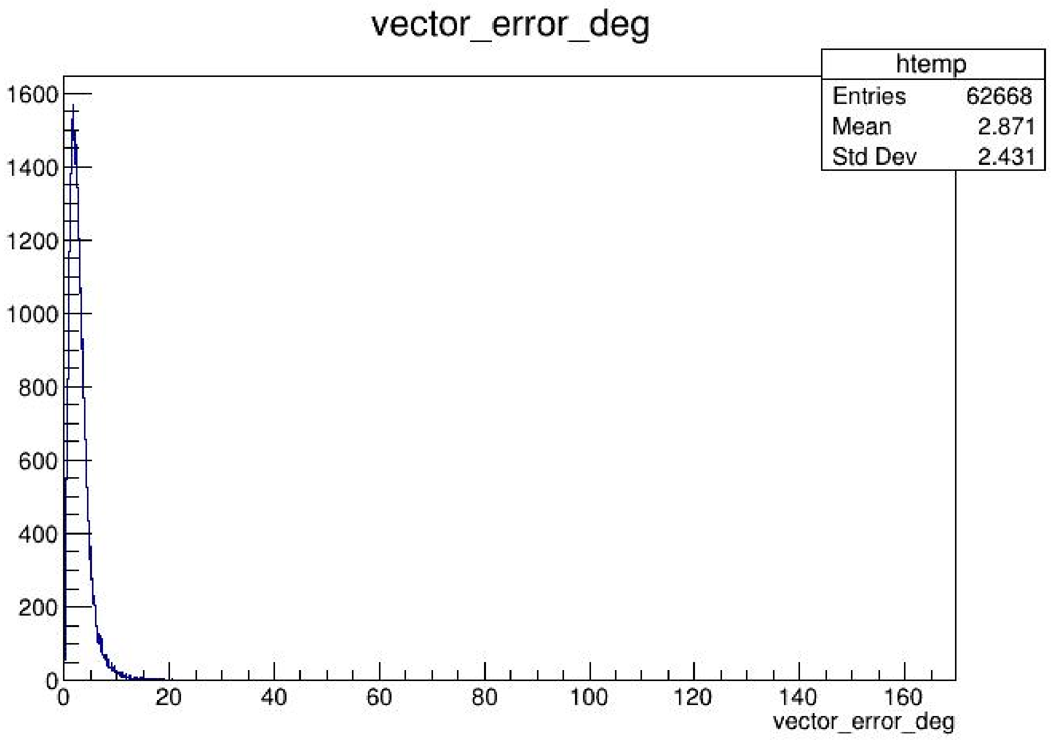

68th percentile:3.21°

The model controls the 3D pointing deviation within 3.21° for 68% of the events, with an average deviation of 2.87°.

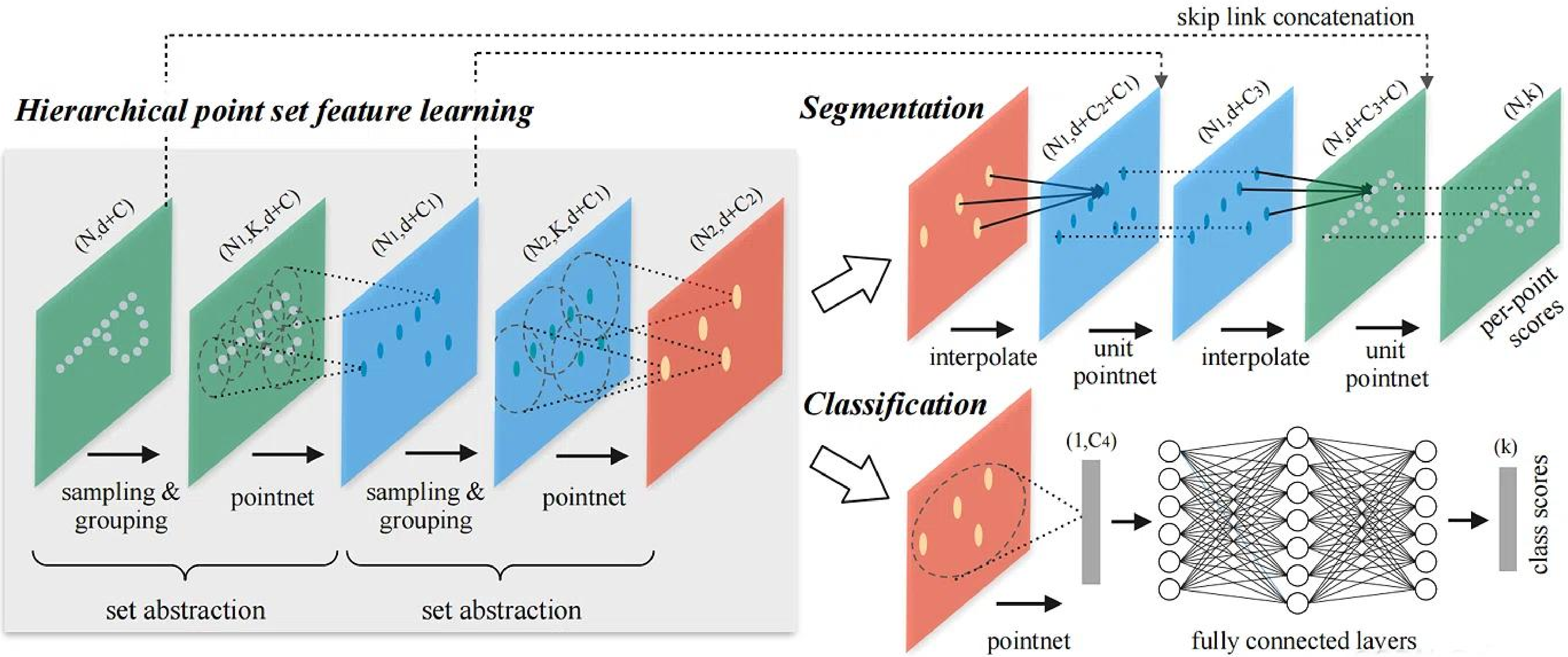
skip link concatenation
Hierarchical point set feature learning
(N,d+C)
(N1,K,d+C)
(N1,d+C1)
(N2,K,d+C1)
(N2,d+C2)
sampling & grouping
pointnet
sampling & grouping
pointnet
set abstraction
set abstraction
Segmentation
(N1,d+C2+C1)
(N1,d+C3)
(N,d+C3+C)
(N,k)
interpolate
unit pointnet
interpolate
unit pointnet
per-point scores
Classification
(1,C4)
(k)
pointnet
fully connected layers
class scores

PointNet++ 3D Angle Prediction Error Analysis

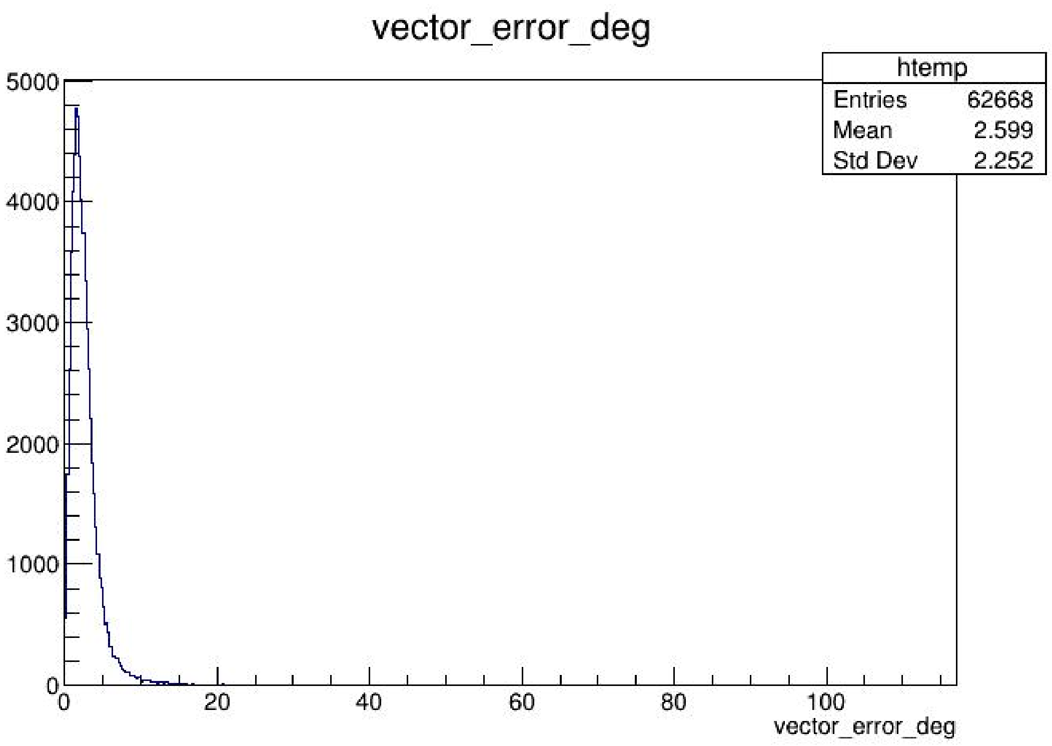

68th percentile:2.86 °

The model controls the 3D pointing deviation within 2.86° for 68% of the events, with an average deviation of 2.60°.

Comparative Reconstruction Accuracy of ML Models

	theta_error_MAE	phi_error_MAE	vector_error_68%	Vector_error_mean
DT	4.86°	8.70°	9.09°	8.34°
RF	3.07°	4.52°	4.93°	4.64°
MLP	2.31°	3.91°	4.08°	3.83°
CNN	1.97°	3.58°	3.95°	3.46°
H-CNN	2.26°	3.52°	3.92°	3.54°
GNN	2.40°	3.80°	4.15°	3.79°
DeepSphere	1.82°	2.83°	3.21°	2.87°
Pointnet++	1.66°	2.60°	2.86°	2.60°

4 Muon Direction Reconstruction Based on Measured Experimental Data

Measured data acquisition

- **Muons enter from the top**
- **Vertical(θ = 0°)has the highest flux**
- **Flux decreases as θ increases toward 90°**

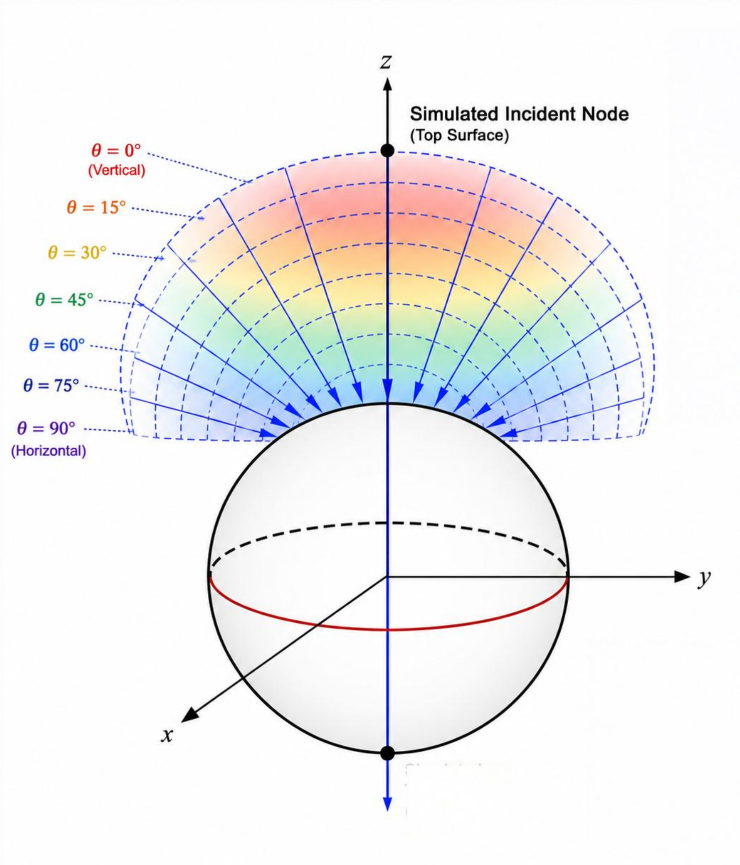

Decision Tree model reconstructs the direction of the measured data

兰州大学 | LANZHOU UNIVERSITY

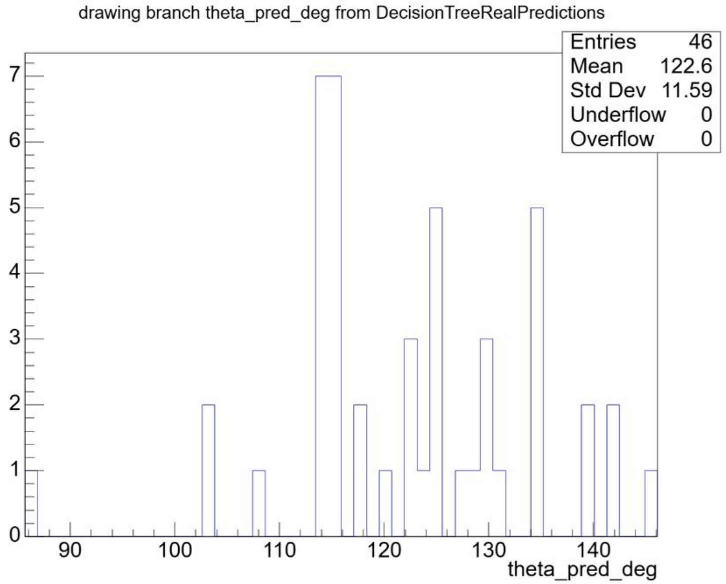

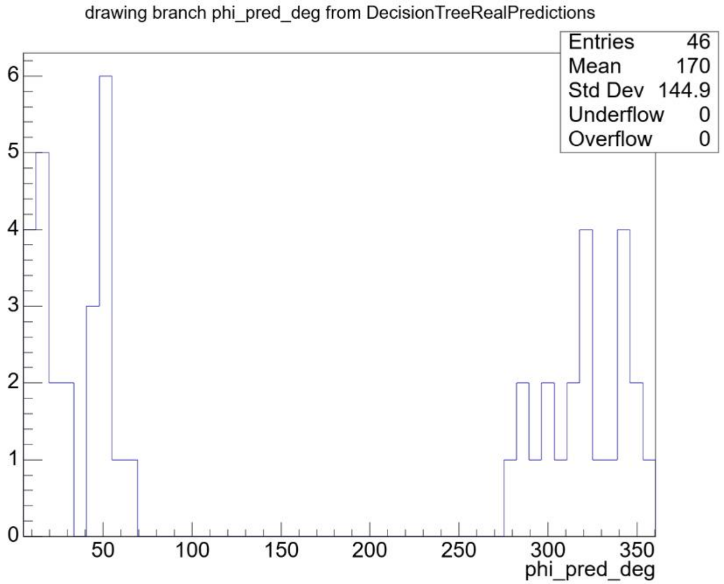

The reconstructed angular distribution deviates significantly from the theoretical expectation. The measured data are incident by the muon from the top of the detector in an angular distribution, and theta angle should show a decreasing distribution from 0 to 90 degrees.

Random forest model reconstructs the direction of the measured data

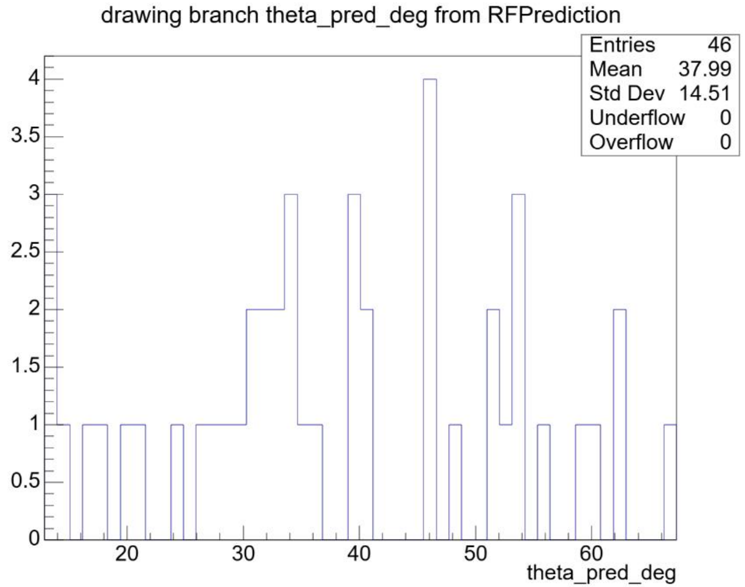

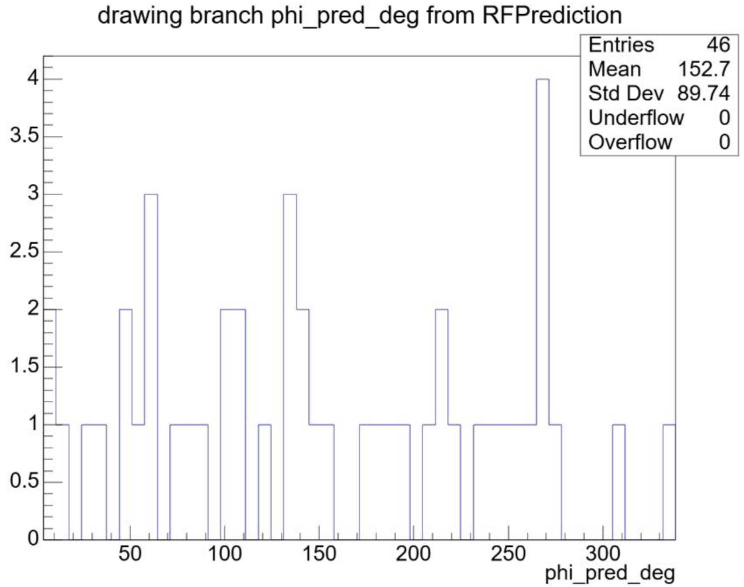

The reconstruction performance remains unsatisfactory, which is attributed to substantial discrepancies between measured and simulated input observables.

Theta reconstruction results of other models for measured data

MLP

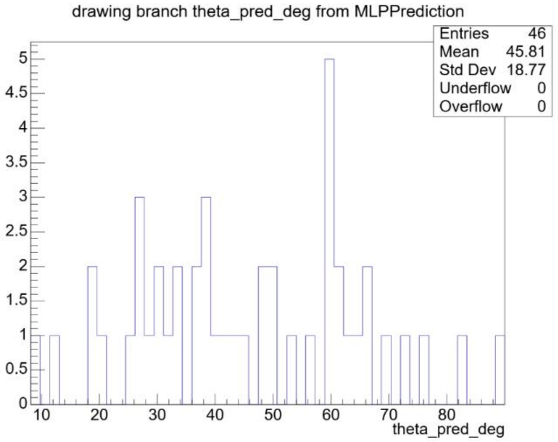

CNN

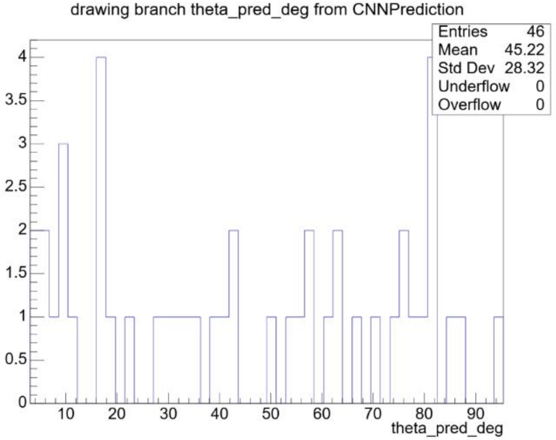

HEALPix-CNN

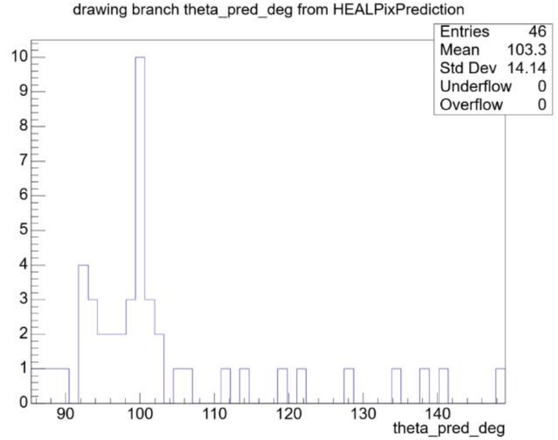

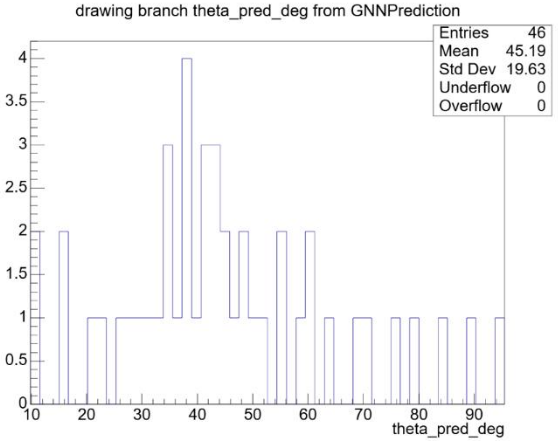

GNN

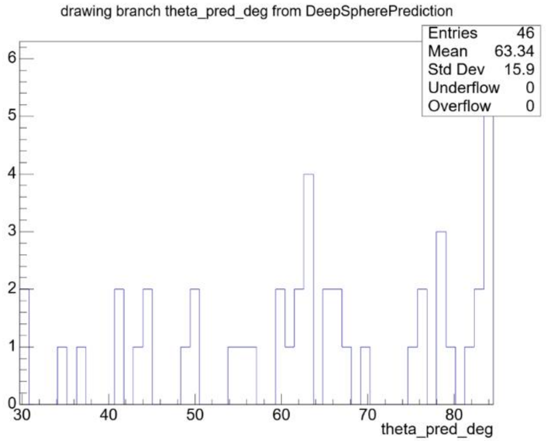

DeepSphere

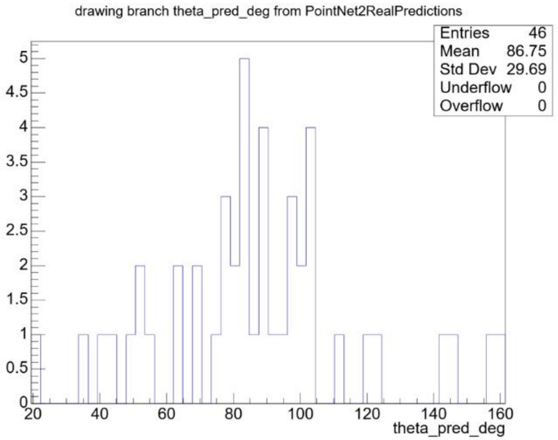

PointNet++

Comparative Reconstruction Accuracy of ML Models(T)

	theta_error_MAE	phi_error_MAE	Vector_error_mean
DT	7.92°	19.58°	16.39°
RF	6.17°	8.64°	9.01°
MLP	3.81°	6.51°	6.32°
CNN	3.12°	5.05°	5.02°
H-CNN	3.89°	6.31°	6.20°
GNN	4.69°	8.58°	8.08°
DeepSphere	3.31°	5.21°	5.25°
Pointnet++	3.01°	5.25°	4.94°

Decision Tree model reconstructs the direction of the measured data

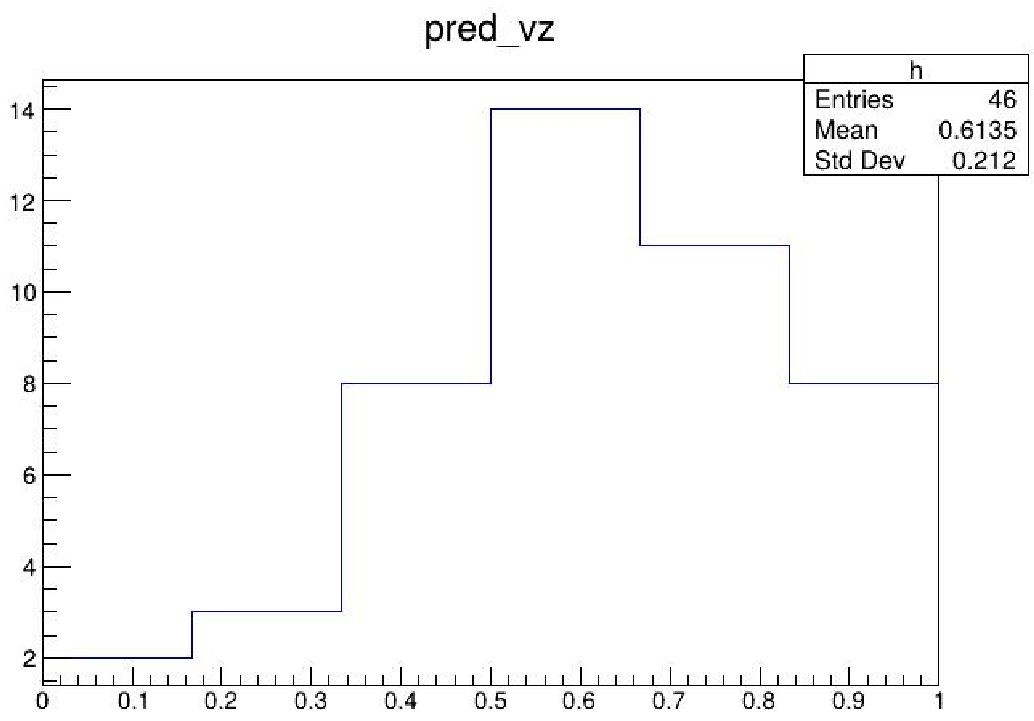

costheta

There is an upward trend and the range is (0, 1).

Random Forest model reconstructs the direction of the measured data

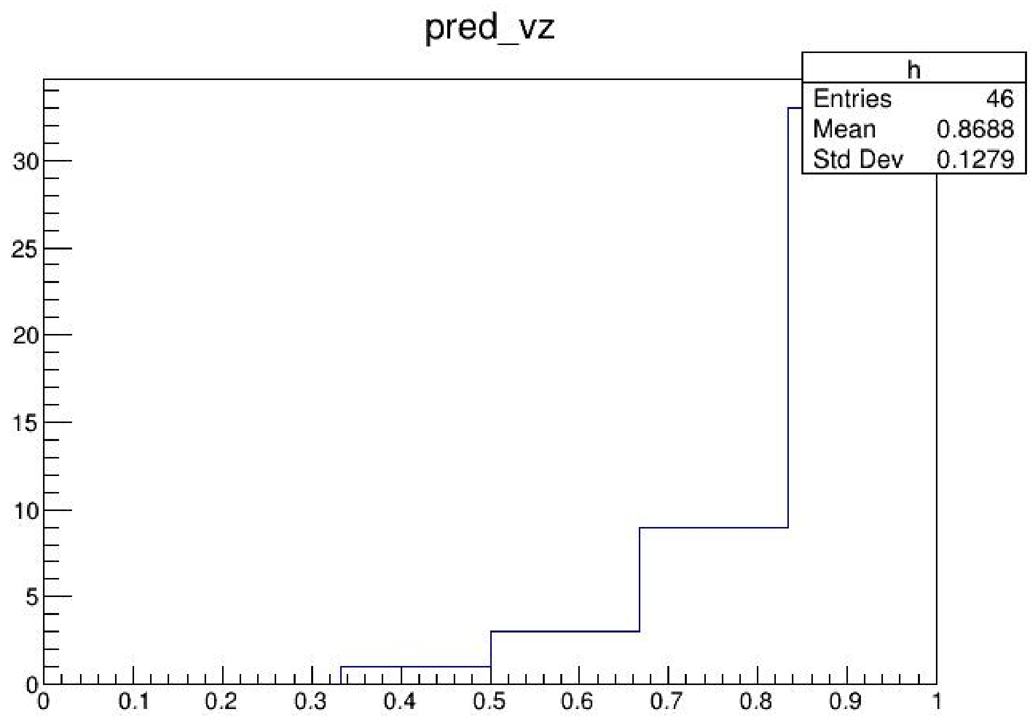

costheta

MLP model reconstructs the direction of the measured data

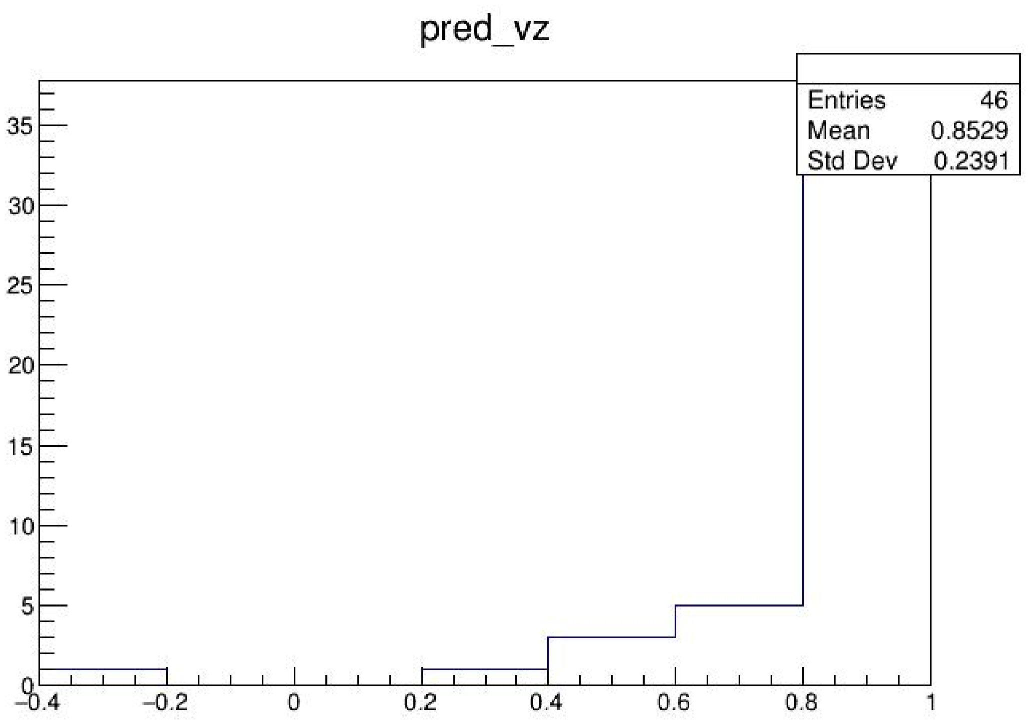

costheta

CNN model reconstructs the direction of the measured data

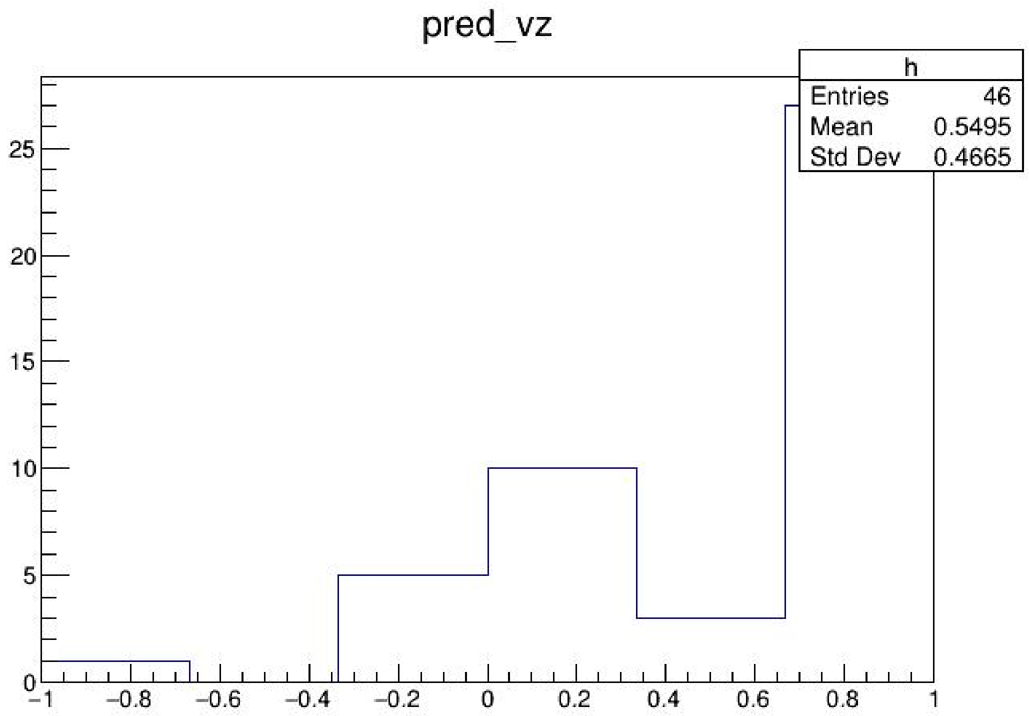

costheta

CNN and MLP are planar structures, which cannot automatically learn the feature that the 0th ring is the ' top '. It treats the ring as a local texture pattern, lacks global symbol constraints, and may predict a small number of negative values.

HEALPix-CNN model reconstructs the direction of the measured data

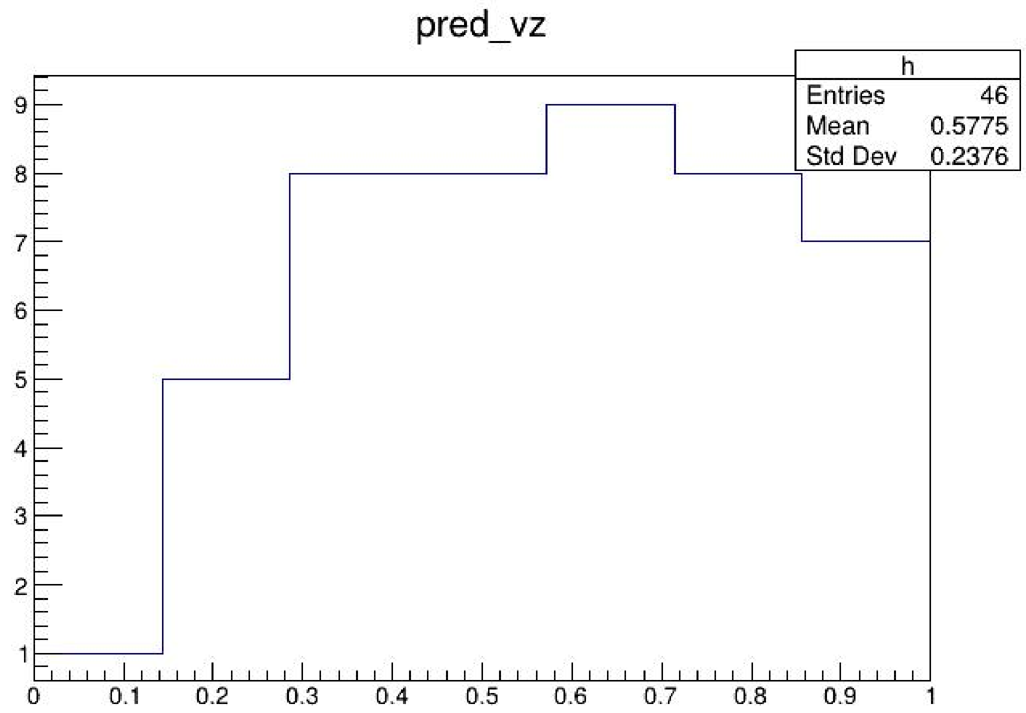

costheta

Directly map the PMT data to the HEALPix spherical pixels. HEALPix pixels have well-defined longitude and latitude coordinates on the sphere, and when using the NESTED arrangement, the pixel continuity strictly follows the spherical hierarchical structure broussonetia papyrifera.

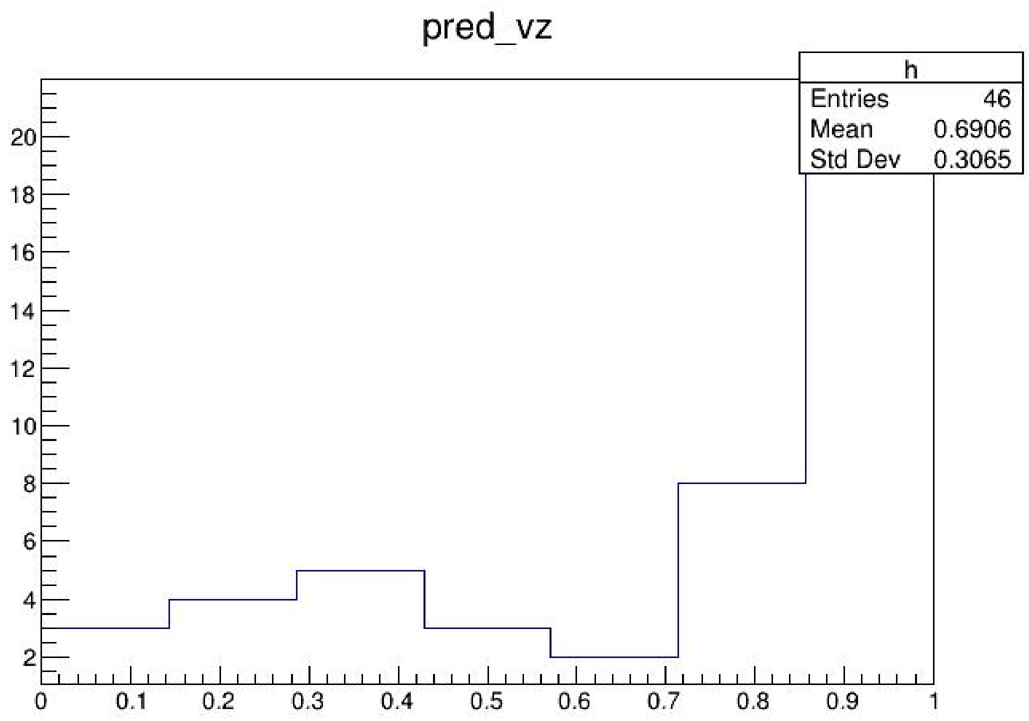
pred_vz
h
Entries 46
Mean 0.6906
Std Dev 0.3065
20
18
16
14
12
10
8
6
4
2
0
0.1
0.2
0.3
0.4
0.5
0.6
0.7
0.8
0.9
1

costheta

Deepsphere model reconstructs the direction of measured data

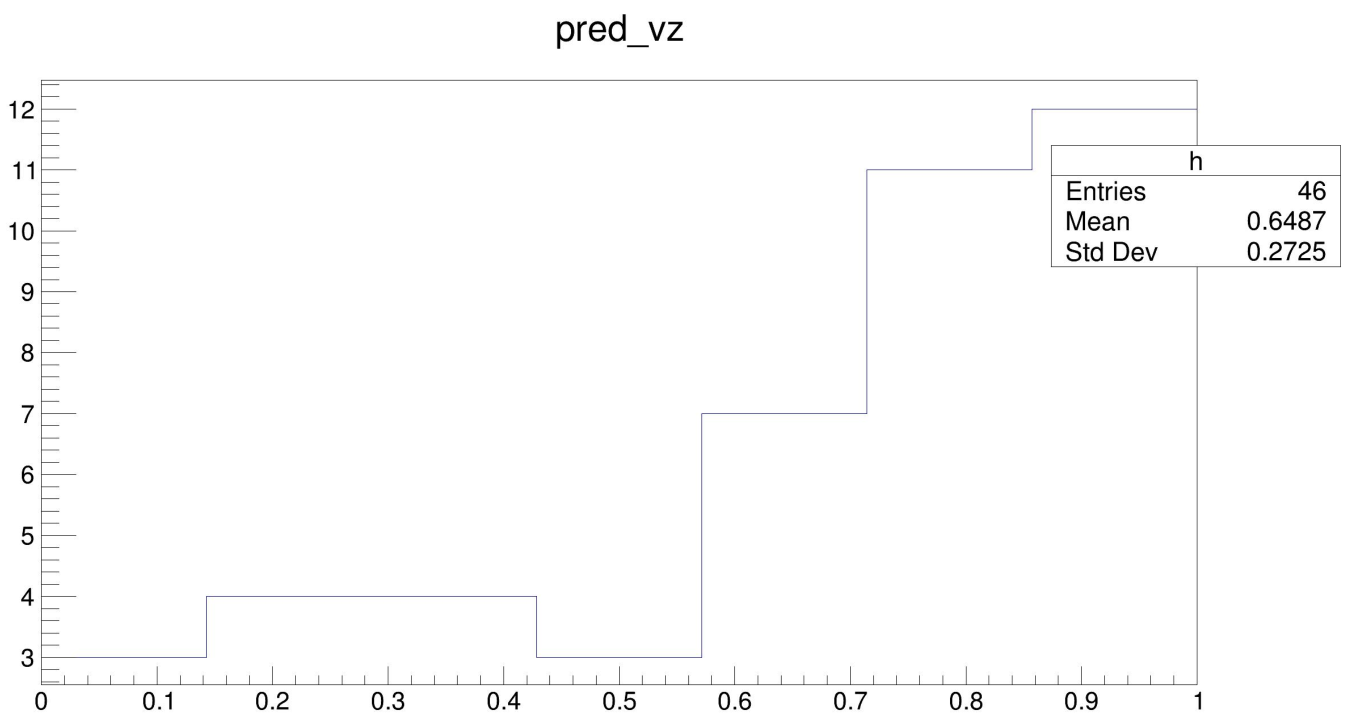

costheta

Pointnet + + model reconstructs the direction of measured data

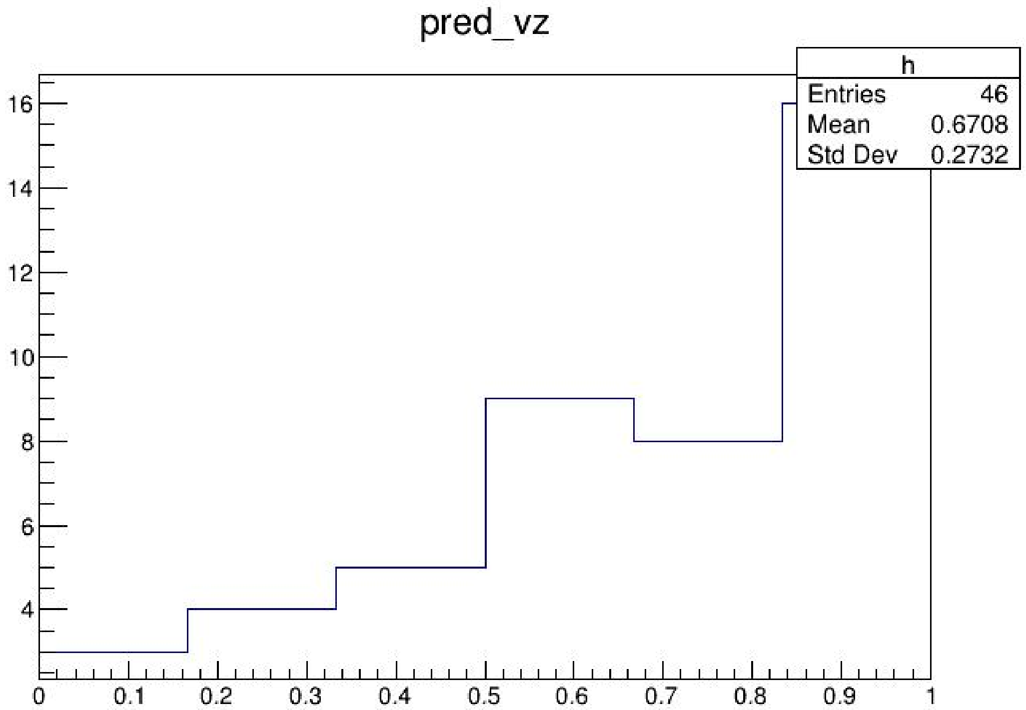

costheta

When only the time observable T is fed into the model as the sole input, the predicted angular distribution matches the real muon incident distribution well. This demonstrates valid acquisition and preprocessing of the measured time signals. In contrast, anomalous charge Q measurements originate from PMT hardware damage or improper waveform processing for charge integration.

5 Conclusion and Future Work

Conclusion and Future Work

兰州大学 | LANZHOU UNIVERSITY

- **Muon event simulation and dataset preprocessing** have been completed, with two key physical observables extracted: trigger time T and deposited charge Q.
- Subsequently, **eight machine learning** (ML) architectures are developed to construct a **muon incident direction prediction model**, followed by full network architecture setup and training.
- The **error distribution** of each model is fitted and systematically analyzed, which quantitatively confirms favorable **angular reconstruction precision and stability**.
- However, the **charge integral channel** of measured data presents severe anomalies induced by **PMT saturation and hardware damage.** To evaluate model performance under defective input observables, only the time feature T is adopted as the sole input to test the ML-based direction reconstruction on experimental data. Calibrated measured datasets will be utilized for subsequent comprehensive validation in follow-up studies.

Thanks

兰州大学 | LANZHOU UNIVERSITY

自强不息 独树一帜

THANKS

LANZHOU UNIVERSITY